Technical Section

A new construction of smooth surfaces from triangle meshes using parametric pseudo-manifolds

Marcelo Siqueira [a,1], Dianna Xu [b,*], Jean Gallier [c], Luis Gustavo Nonato [d,e,2], Dimas Martínez Morera [f], Luiz Velho [g]

[a] *UFMS, Campo Grande (MS), Brazil*
[b] *Department of Computer Science, Bryn Mawr College, Bryn Mawr, PA 19067, USA*
[c] *University of Pennsylvania, Philadelphia (PA), USA*
[d] *ICMC-USP, São Carlos (SP), Brazil*
[e] *Scientific Computing and Imaging Institute, University of Utah, Salt Lake City (UT), USA*
[f] *UFAL, Maceió (AL), Brazil*
[g] *IMPA, Rio de Janeiro (RJ), Brazil*

ARTICLE INFO

ABSTRACT

We introduce a new manifold-based construction for fitting a smooth surface to a triangle mesh of arbitrary topology. Our construction combines in novel ways most of the best features of previous constructions and, thus, it fills the gap left by them. We also introduce a theoretical framework that provides a sound justification for the correctness of our construction. Finally, we demonstrate the effectiveness of our manifold-based construction with a few concrete examples.

© 2009 Elsevier Ltd. All rights reserved.

1. Introduction

The problem of fitting a surface with guaranteed topology and continuity to the vertices of a polygonal mesh of arbitrary topology has been a topic of major research interest for many years. The main difficulty of this problem lies in the fact that, in general, meshes of arbitrary topology cannot be parametrized on a single rectangular domain and have no restriction on vertex connectivity. Most existing solutions rely on mathematical and computational frameworks capable of guaranteeing low orders (i.e., C^2 and below) of continuity only. However, higher order surfaces are often required for certain numerical simulations and to meet visual, aesthetic, and functional requirements. While a few high order constructions do exist, most are expensive, complex, and/or difficult to implement.

Much of the previous research efforts has been focused on stitching parametric polynomial patches together along their seams, where each patch is the image of a distinct parametrization of a closed, planar domain. Because the patches need to be "pieced" together, ensuring continuity along the borders has proved to be a difficult problem, particularly for closed meshes. Although there is a large number of C^k/G^k constructions based on the "stitching" paradigm and catered to triangle meshes [1], only very few go beyond C^2-continuity [2,3]. Existing constructions (even those C^2 and below) are typically complex, and they lack shape control and cannot achieve good visual quality without additional processing. Very few were ever implemented and the degree of the polynomial patches required by most constructions grows with the desired order of continuity, which tend to yield surfaces with poor visual quality.

Subdivision surface is another popular approach which has been extensively investigated in the past 30 years [4–10]. These techniques are intuitive, simple to implement and in general produce smooth surfaces of good visual quality. However, constructions that go beyond C^2/G^2 are rare, and guaranteeing continuity around *extraordinary* vertices is difficult [11,12]. Furthermore, previous efforts by Prautzsch and Reif [13,14] indicate that subdivision schemes to produce C^k surfaces, for $k \geqslant 2$, cannot be as simple and elegant as existing C^1/G^1 subdivision schemes.

Unlike the two aforementioned approaches, the manifold-based approach pioneered by Grimm and Hughes [15] has proved well suited to fit, with relative ease, C^k-continuous parametric surfaces to triangle and quadrilateral meshes, including $k = \infty$ [15–19]. The mathematical theory of manifolds was conceived

* Corresponding author. Tel.: +16105266502; fax: +16105267469.
E-mail addresses: marcelo@dct.ufms.br (M. Siqueira), dxu@cs.brynmawr.edu (D. Xu), jean@cis.upenn.edu (J. Gallier), gnonato@icmc.usp.br (L.G. Nonato), dimas@mat.ufal.br (D.M. Morera), lvelho@impa.br (L. Velho).

with built-in arbitrary smoothness, and the differential structure of a manifold provides us with a natural setting for solving equations on surfaces. Manifold-based constructions also share some of the most important properties of splines surfaces, such as local shape control and fixed-sized local support for basis functions. Thus, as pointed out by Grimm and Zorin [20], a manifold is an attractive surface representation form for a handful of applications in graphics, such as reaction–diffusion texture, texture synthesis, fluid simulation, and surface deformation.

Unfortunately, existing manifold-based constructions present some drawbacks that limit their wide use in practical applications. In particular, constructions able to handle triangle meshes either make use of an intricate mechanism to define the manifold structure [15,19] or produce surfaces with singular (i.e., extraordinary) points [18], which must be removed either at the expense of reduced continuity around those points or the resulting surface being not entirely polynomial (if exponential functions are used). On the other hand, methods with a simpler construction [16] as well as arbitrary smoothness [17] do not establish a complete framework for handling triangle meshes.

1.1. Contributions

The contributions of this paper are twofold:

1. We introduce a new manifold-based construction for fitting surfaces of arbitrary smoothness (i.e., C^∞-continuous) to triangle meshes. Our construction combines, in the same framework, *most* of the best features of previous constructions. In particular, it is more compact and simpler than the ones in [15,19], does not contain singular points as the construction in [18], and shares with [17], a construction devised for quadrilateral meshes, the ability of producing C^∞-continuous surfaces and the flexibility in ways of defining the geometry of the resulting surface.
2. We also briefly describe a theoretical framework that provides a sound justification for the correctness of our manifold-based construction. This framework is an improvement upon the one developed by Grimm and Hughes [15], which was used to undergird the constructions described in [15–17,19].

2. Prior work

Extensive literature exists on fitting smooth surfaces from meshes. However, in order to better contextualize our approach, we focus this section on manifold-based techniques. For a more detailed review of the manifold-based approach and its applications, we refer the reader to [20].

The first manifold-based construction for surface modeling was proposed by Grimm and Hughes [15]. Their seminal work has since then been the basis of most subsequent constructions, including ours. Their construction takes a triangle mesh as input, subdivides by one step of Catmull–Clark subdivision scheme, and then considers the dual of the subdivided mesh (which is no longer a triangle mesh). Surface topology is defined from a structure they named *proto-manifold*, which contains a finite set A of connected open sets in $\mathbb{R}^2$ (the theory holds in $\mathbb{R}^n$ indeed) and a set of transition functions that, together with the mesh connectivity, dictate how the sets in A overlap with each other. Each type of mesh element (vertex, edge, and face) gives rise to a different open set, requiring the construction of three different types of transition functions. Geometry is added by handling the mesh geometry through control points and blending functions explicitly defined from the open sets. The construction in [15] yields C^2-continuous surfaces only, but it was later simplified and

improved [21] to produce C^k-continuous surfaces, for any finite integer k. Subsequent efforts [16,17] aimed at providing a construction that requires a smaller set of open sets, consists of simpler transition functions, and achieves C^∞-continuity.

Based on the concept of proto-manifold, Navau and Pla-Garcia [16] introduced a construction that takes a quadrilateral mesh and two integers, k and n, as input. The integer k specifies the desired degree of (finite) continuity, while n is related to the extent of the open sets in A. Their construction assigns an open set to each mesh vertex. Differently from [15], only two types of open sets are built, one associated with regular vertices (valence equal 4) and the other with irregular vertices. However, three distinct types of transition functions are still needed so as to glue regular–regular, regular–irregular, and irregular–irregular open sets. The size of the set A grows with n, but it also depends on the mesh topology. In fact, it can be larger than the size of A in [15] even for smaller values of n. Geometry is defined quite similarly as in [15]. An extension of [16] to meshes of arbitrary topology has been proposed [22], but it shares with the construction in [16] the same advantages and drawbacks.

Ying and Zorin [17] devised a very elegant proto-manifold structure from quadrilateral meshes. Making use of only one type of open set and a simple analytical transition function, the resulting surface is C^∞-continuous. This work improves upon the two previous techniques considerably. Another contribution is that control points are replaced by general polynomials, thus offering a more flexible control of the geometry of the resulting surface. Their construction can be extended to deal with triangle meshes, but one has to work out certain elements of its proto-manifold, which are not entirely obvious.

Gu et al. [18] introduced a triangle-based manifold construction called *manifold splines*, which is based on a theoretical framework of its own. This construction employs affine transforms as transition functions and (rational) polynomial functions to derive the geometry. This is the first manifold-based construction to yield a purely (rational) polynomial surface. Manifold splines are in general more compact to represent and cheaper to evaluate than the surfaces produced by any other construction (including ours). However, as closed surfaces (except tori) cannot be covered by an "affine atlas" (see [23]), singular points not belonging to any open set of the atlas must appear on the surface. These points are removed and traditional spline hole-filling techniques are used, which may affect the visual quality of the surface in the vicinity of the holes. Making use of discrete Ricci flow, Gu et al. [24] have simplified and improved the manifold spline construction to reduce to only one singular point on the entire surface.

Very recently, Vecchia et al. [19] introduced another triangle-based manifold construction, which also represents the resulting surface with a rational polynomial. However, unlike the constructions in [18,24], the surface does not contain any singular points. Unfortunately, the construction in [19] suffers from the same problem as the one in [15]: it makes use of an intricate mechanism to define its transition functions and their domains. In addition, the construction is not theoretically guaranteed to build C^k surfaces, for any finite k, although experimental evidence indicates that it does.

Our construction is based on the theoretical framework developed by Grimm and Hughes [15], yet it differs from the aforementioned constructions in the following aspects: the proto-manifold counterpart of our construction is given two additional conditions that render it stronger and more general than the proto-manifold in [15]. As in [17], our construction also has only one type of open set and (simple) transition function, can produce C^∞ surfaces, and defines the geometry of the resulting surfaces using polynomials. Differently from Ying and Zorin [17], our

construction is devised to work with triangle meshes, which are far more popular than quadrilateral meshes in graphics applications [25]. In addition, we define geometry from simpler polynomials (i.e., rectangular Bézier patches) which means that the resulting surface is contained in the convex hull of all control points defining its patches. This property allows us to optimize for speed ray tracing and collision detection algorithms. The surfaces produced by our construction are not polynomial, but they do not contain any singular points. Finally, our construction appears simpler to implement than the ones given in [15,16,18,24,19].

3. Mathematical background

The formal definition of a manifold can be found in standard mathematics textbooks, such as [26]. Informally, manifolds are spaces that locally behave like the familiar n-dimensional Euclidean space, and on which we can do calculus (e.g., compute derivatives, integrals, volumes, and curvatures). For that, each manifold, $\mathcal{M}$, is equipped with an *atlas*, which is a collection of *charts*. Each chart is a pair (U, φ), where U is an open set of $\mathcal{M}$ and $\varphi : U \to \varphi(U) \subseteq \mathbb{R}^n$ is a homeomorphism. Furthermore, the charts of an atlas must cover $\mathcal{M}$. The open sets, U_1 and U_2, of any two distinct charts, (U_1, φ_1) and (U_2, φ_2), may overlap (see Fig. 1). *Transition functions*, $\varphi_{21} : \varphi_1(U_1 \cap U_2) \to \varphi_2(U_1 \cap U_2)$ and $\varphi_{12} : \varphi_2 (U_1 \cap U_2) \to \varphi_1(U_1 \cap U_2)$, are defined to move between the overlapped regions consistently. These functions are required to satisfy two conditions: $\varphi_{21} = \varphi_2 \circ \varphi_1^{-1}$ and $\varphi_{12} = \varphi_1 \circ \varphi_2^{-1}$. Basically, functions φ_{21} and φ_{12} define which points in $\varphi_1(U_1 \cap U_2)$ and $\varphi_2(U_1 \cap U_2)$ correspond to the same point in $\mathcal{M}$ under φ_1^{-1} and φ_2^{-1}. Transition functions are often required to be C^k-continuous, so that the necessary degree of "smoothness" to compute differential properties is ensured.

A manifold-based approach for surface construction requires first building a manifold, $\mathcal{M}$, which is a smooth surface in $\mathbb{R}^3$. The classic definition of a manifold assumes the existence of a manifold *a priori*, which is not very helpful from the constructive point of view. Fortunately, it is possible to define $\mathcal{M}$ in a constructive manner from a set of *gluing data* and a set of *parametrizations*.

Definition 1. Let n be an integer with $n \geqslant 1$ and let k be either an integer with $k \geqslant 1$ or $k = \infty$. A *set of gluing data* is a triple,

$$\mathcal{G} = ((\Omega_i)_{i \in I}, (\Omega_{ij})_{(ij) \in I \times I}, (\varphi_{ji})_{(i,j) \in K}),$$

satisfying the following properties, where I and K are (possibly infinite) countable index sets, and I is non-empty:

1. For every $i \in I$, the set Ω_i is a non-empty open subset of $\mathbb{R}^n$ called *parametrization domain*, for short, *p-domain*, and the Ω_i are pairwise disjoint (i.e., $\Omega_i \cap \Omega_j = \emptyset$ for all $i \neq j$).
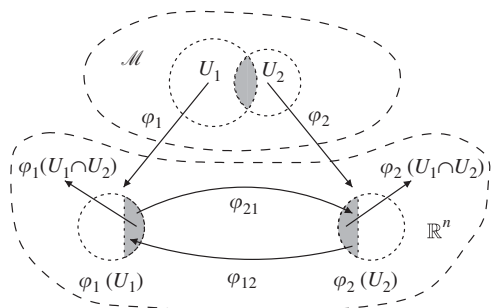
2. For every pair $(i,j) \in I \times I$, the set Ω_{ij} is an open subset of Ω_i. Furthermore, $\Omega_{ii} = \Omega_i$ and $\Omega_{ji} \neq \emptyset$ if and only if $\Omega_{ij} \neq \emptyset$. Each non-empty Ω_{ij} (with $i \neq j$) is called a *gluing domain*.

3. If we let

$$K = \{(i,j) \in I \times I | \Omega_{ij} \neq \emptyset\},$$

then $\varphi_{ji} : \Omega_{ij} \to \Omega_{ji}$ is a C^k bijection for every $(i,j) \in K$ called a *transition function* (or *gluing function*) and the following conditions hold:

(a) $\varphi_{ii} = \mathrm{id}_{\Omega_i}$, for all $i \in I$,

(b) $\varphi_{ij} = \varphi_{ji}^{-1}$, for all $(i,j) \in K$, and

(c) For all i, j, k, if $\Omega_{ji} \cap \Omega_{jk} \neq \emptyset$, then $\varphi_{ji}^{-1}(\Omega_{ji} \cap \Omega_{jk}) \subseteq \Omega_{ik}$ and $\varphi_{ki}(x) = \varphi_{kj} \circ \varphi_{ji}(x)$, for all $x \in \varphi_{ji}^{-1}(\Omega_{ji} \cap \Omega_{jk})$.

4. For every pair $(i,j) \in K$, with $i \neq j$, for every $x \in \partial(\Omega_{ji}) \cap \Omega_i$ and $y \in \partial(\Omega_{ji}) \cap \Omega_j$, there are open balls, V_x and V_y, centered at x and y, so that no point of $V_y \cap \Omega_{ji}$ is the image of any point of $V_x \cap \Omega_{ij}$ by φ_{ji}.

There is a direct correspondence between some of the constituents of the traditional definition of a manifold and the constituents of a set of gluing data (refer to Fig. 2):

- each *p-domain*, $\Omega_i \subseteq \mathbb{R}^n$, is the image, $\Omega_i = \varphi_i(U_i)$, of an open set, U_i, of $\mathcal{M}$ under the map φ_i of the chart (U_i, φ_i) of an atlas of $\mathcal{M}$;

- each *gluing domain*, $\Omega_{ij} \subseteq \Omega_i$, is the image, $\Omega_{ij} = \varphi_i(U_i \cap U_j)$, of the overlapping subset, $U_i \cap U_j$, of U_i and U_j under the map φ_i of the chart (U_i, φ_i) of an atlas of $\mathcal{M}$;

- each *transition function*, $\varphi_{ij} : \Omega_{ji} \to \Omega_{ij}$, is a function from $\varphi_j(U_i \cap U_j) = \Omega_{ji}$ to $\varphi_i(U_i \cap U_j) = \Omega_{ij}$.

Condition 3(c) is called the *cocycle condition* and it plays a crucial role in Theorem 1, which states that an n-dimensional C^k manifold can be constructed from a set of gluing data. The idea behind the proof of Theorem 1 is to define a *set of parametrizations*, $(\theta_i)_{i \in I}$, such that (1) each

$$\theta_i : \Omega_i \to \theta_i(\Omega_i)$$

is a C^k homeomorphism associated with a *p-domain*, Ω_i, of the given set of gluing data, and (2) the union set,

$$\bigcup_{i \in I} \theta_i(\Omega_i),$$

admits a C^k n-dimensional atlas whose charts are the pairs $(\theta_i(\Omega_i), \varphi_i)$, with $\varphi_i = \theta_i^{-1}$ (see Figs. 1 and 2).

As customary in mathematics, one in general assumes some extra conditions on a manifold in order to be able to do mathematical analysis with it. A very common choice is to require that the manifold be Hausdorff. Condition 4 of Definition 1 ensures that a Hausdorff manifold can always be constructed from a set of gluing data. It turns out that this condition is necessary and sufficient [27].
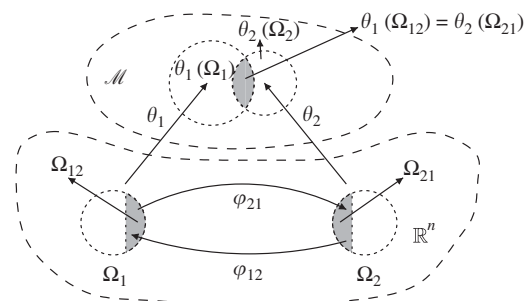

Fig. 1. Constituents of a manifold.

Fig. 2. Constituents of a parametric pseudo-manifold.

Theorem 1. *For every set of gluing data,*

$$\mathscr{G} = ((\Omega_i)_{i\in I}, (\Omega_{ij})_{(i,j)\in I\times I}, (\varphi_{ji})_{(i,j)\in K}),$$

there is an n-dimensional C^k manifold, $M_{\mathscr{G}}$, whose transition functions are the φ_{ji}'s.

Proof. See [27] for a proof. □

Unfortunately, our proof of Theorem 1 gives us a theoretical construction, which yields an "abstract" manifold, $M_{\mathscr{G}}$, but no information on the geometry of this manifold. Furthermore, $M_{\mathscr{G}}$ may not be orientable or compact. However, for the problem we are dealing with, we are given a triangle mesh and we want to build a "concrete" manifold: a surface in $\mathbb{R}^3$ that approximates the given mesh. It turns out that it is always possible to define a *parametric pseudo-manifold* from any given set of gluing data, whose *image* in $\mathbb{R}^3$ is a surface if certain conditions hold.

Definition 2. Let n and d be two integers with $n > d \geqslant 1$ and let k be integer with $k \geqslant 1$ or $k = \infty$. A *parametric C^k pseudo-manifold of dimension d in $\mathbb{R}^n$, $\mathcal{M}$,* is a pair

$$\mathcal{M} = (\mathscr{G}, (\theta_i)_{i\in I}),$$

where $\mathscr{G} = ((\Omega_i)_{i\in I}, (\Omega_{ij})_{(i,j)\in I\times I}, (\varphi_{ji})_{(i,j)\in K})$ is a set of gluing data, for some finite set I, and each θ_i is a C^k function, $\theta_i : \Omega_i \to \mathbb{R}^n$, called a *parametrization* such that

$$\theta_i = \theta_j \circ \varphi_{ji},$$

for all $(i,j) \in K$. The subset, $M \subset \mathbb{R}^n$, given by

$$M = \bigcup_{i\in I} \theta_i(\Omega_i)$$

is called the *image* of the parametric pseudo-manifold, $\mathcal{M}$.

When $d = 2$ and $n = 3$ in Definition 2, we call $\mathcal{M}$ a *parametric pseudo-surface* (PPS). If we require the θ_i's to be bijective and to further satisfy the two conditions

$$\theta_i(\Omega_i) \cap \theta_j(\Omega_j) = \theta_i(\Omega_{ij}) = \theta_j(\Omega_{ji}), \quad \text{for all } (i,j) \in K,$$

and

$$\theta_i(\Omega_i) \cap \theta_j(\Omega_j) = \emptyset, \quad \text{for all } (i,j) \notin K,$$

then the image, M, of the PPS, $\mathcal{M}$, is guaranteed to be a surface in $\mathbb{R}^3$ [27]. The following remarks state important facts regarding the theoretical contributions of our work:

Remark 1. There is a subtle and yet important difference between our definition of a set of gluing data (i.e., Definition 1) and the definition of a proto-manifold in [15]: our cocycle condition (condition 3(c) of Definition 1) is stronger than the one in [15], as the latter does not always guarantee that a (valid) manifold can be constructed from a proto-manifold (see [27] for a proof).

Remark 2. In the definition of a proto-manifold (see [15]), there is no condition similar to condition 4 above. In order to ensure that the manifold built from a proto-manifold is Hausdorff, a local embedding property of certain gluings is required (see [28]). This requirement is stronger than condition 4, as it prevents us from obtaining certain manifolds such as a 2-sphere resulting from gluing two open discs in $\mathbb{R}^2$ along an annulus.

4. The construction of a PPS

Recall that our goal is to fit a surface, $S \in \mathbb{R}^3$, to a triangle mesh $\mathcal{T}$. More specifically, we want to build a surface S that approximates the vertices of $\mathcal{T}$ and has the same topology as the underlying space, $|\mathcal{T}|$, of $\mathcal{T}$ (i.e., $|\mathcal{T}|$ is the point set resulting from the union of all points comprising the vertices, edges, and triangles of $\mathcal{T}$). We also assume that $|\mathcal{T}|$ is a surface in $\mathbb{R}^3$ with

empty boundary. Finally, to build S, our construction defines a set of gluing data and a set of parametrizations of a PPS.

The set of gluing data,

$$\mathscr{G} = ((\Omega_i)_{i\in I}, (\Omega_{ij})_{(i,j)\in I\times I}, (\varphi_{ji})_{(i,j)\in K}),$$

is defined from the elements of $\mathcal{T}$, while the set of parametrizations, $(\theta_i)_{i\in I}$, where $\theta_i : \Omega_i \to \theta(\Omega_i) \subset \mathbb{R}^3$, for every $i \in I$, is defined from $|\mathcal{T}|$. The key idea is to define a PPS,

$$\mathcal{M} = (\mathscr{G}, (\theta_i)_{i\in I}),$$

such that the image,

$$S = \bigcup_{i\in I} \theta_i(\Omega_i),$$

of $\mathcal{M}$ in $\mathbb{R}^3$ is a surface, $S \subset \mathbb{R}^3$, that approximates $|\mathcal{T}|$. In what follows we describe how to build $\mathscr{G}$ and $(\theta_i)_{i\in I}$.

4.1. Building a set of gluing data

Let

$$I = \{u \mid u \text{ is a vertex of } \mathcal{T}\}.$$

To build the set of gluing data, $\mathscr{G}$, we must define its collection of *p*-domains, gluing domains, and transition functions. These collections are defined in terms of two abstractions, a P-polygon and its canonical triangulation, and a composite bijective function. Before we describe these elements, we make a remark regarding our notation:

Remark 3. Each element to be defined next is either related to a vertex, u, or to an edge, $[u, v]$, of $\mathcal{T}$. So, we use the subscript u (e.g., as in Ω_u), to denote an element related to vertex u, and the subscripts (u, v), (v, u), uv, or vu (e.g., as in Ω_{uv} and Ω_{vu}) to denote two elements related to $[u, v]$.

Definition 3. For every $u \in I$, the *p-domain* Ω_u is the set

$$\Omega_u = \{(x, y) \in \mathbb{R}^2 \mid x^2 + y^2 < [\cos(\pi/m_u)]^2\},$$

where m_u is the valence of vertex u. For any two $u, v \in I$, we assume that Ω_u and Ω_v belong to distinct "copies" of $\mathbb{R}^2$. So, $\Omega_u \cap \Omega_v = \emptyset$, and condition 1 of Definition 1 holds.

To build gluing domains and transition functions, we define the notions of a P-polygon and its canonical triangulation, as well as a bijective function that is a composition of two rotations, an analytic function, and a double reflection. For each vertex u of $\mathcal{T}$, the *P-polygon, P_u*, associated with u is the regular polygon in $\mathbb{R}^2$ given by the vertices

$$u'_i = \left(\cos\left(\frac{2\pi \cdot i}{m_u}\right), \sin\left(\frac{2\pi \cdot i}{m_u}\right)\right),$$

for each $i \in \{0, \ldots, m_u - 1\}$, where m_u is the valence of u (see Fig. 3). We assume that P_u resides in the copy of $\mathbb{R}^2$ that contains the *p*-domain Ω_u. So, Ω_u is the interior, $\text{int}(C_u)$, of the circle, C_u, inscribed in the P-polygon, P_u, i.e., $\Omega_u = \text{int}(C_u)$.

We can triangulate P_u by adding m_u diagonals and the vertex, $u' = (0, 0)$, to P_u. Each diagonal connects u' to a vertex, u'_i, of P_u, for each $i = 0, \ldots, m_u - 1$. The resulting triangulation, denoted by T_u, is called the *canonical triangulation of P_u* (see Fig. 3). Denote the set of vertices of T_u by $V(T_u)$, and let $\mathcal{N}(u, \mathcal{T})$ be the subset of vertices of $\mathcal{T}$ such that $v \in \mathcal{N}(u, \mathcal{T})$ if and only if $v = u$ or v is a vertex connected to u by an edge, $[u, v]$, of $\mathcal{T}$. Then, we can define a bijection, $s_u : \mathcal{N}(u, \mathcal{T}) \to V(T_u)$, such that $s_u(u) = u'$ and $[u, u_i, u_{i+1}]$ is a triangle in $\mathcal{T}$ if and only if $[s_u(u) = u', s_u(u_i), s_u(u_{i+1})]$ is a triangle in T_u, where $i = 0, 1, \ldots, m_u - 1$ and $i + 1$ should be considered congruent modulo m_u. We can extend the bijection s_u to map triangles incident to u in $\mathcal{T}$ onto triangles in T_u.
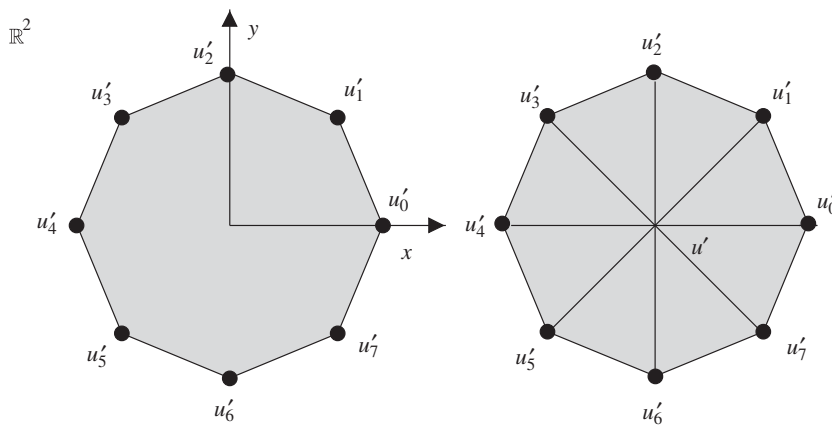
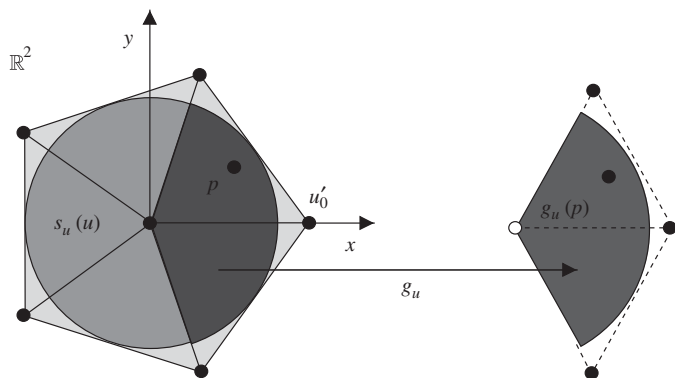**Fig. 3.** A P-polygon (left) and its canonical triangulation (right).

Fig. 4. The action of g_u upon a point $p \in C_u$.

In particular, if $\sigma = [u, u_i, u_{i+1}]$ is a triangle of $\mathcal{T}$ then $s_u(\sigma) = [u', s_u(u_i), s_u(u_{i+1})]$ is its corresponding triangle in T_u. Unless explicitly stated otherwise, we may occasionally denote vertex $s_u(v)$ by v', for every $v \in \mathcal{N}(u, \mathcal{T})$.

For each u in I and for each $p \in \mathbb{R}^2$, with $p \neq (0,0)$, let $g_u : \mathbb{R}^2 - \{(0,0)\} \to \mathbb{R}^2 - \{(0,0)\}$ be given by

$$g_u(p) = \Pi^{-1} \circ f_u \circ \Pi(p),$$

for every $p \in \mathbb{R}^2 - \{(0,0)\}$, where $\Pi : \mathbb{R} \to (-\pi, \pi] \times \mathbb{R}_+$ is the function that converts Cartesian to polar coordinates, and $f_u(-\pi, \pi] \times \mathbb{R}_+ \to (-\pi, \pi] \times \mathbb{R}_+$ is given by

$$f_u(\theta, r) = \left(\frac{m_u}{6} \cdot \theta, \frac{\cos(\pi/6)}{\cos(\pi/m_u)} \cdot r \right), \tag{1}$$

where $(\theta, r) = \Pi(p)$ are the polar coordinates of p. Function g_u has the following interpretation (refer to Fig. 4): it maps the interior of the circular sector, A, of C_u onto the interior of the circular sector, B, of the circle of radius $\cos(\pi/6)$ and centers at $(0,0)$, where A consists of $(0,0)$ and all points with polar coordinates $(\theta, r) \in [-2\pi/m_u, 2\pi/m_u] \times (0, \cos(\pi/m_u)]$ and B consists of $(0,0)$ and all points with polar coordinates $(\beta, s) \in [-\pi/3, \pi/3] \times (0, \cos(\pi/6)]$. We say that B is the *canonical sector*.

Note that g_u is a bijection. Its inverse, g_u^{-1}, is given by

$$g_u(p) = \Pi^{-1} \circ f_u^{-1} \circ \Pi(p),$$

for every $q \in \mathbb{R}^2 - \{(0,0)\}$, where

$$f_u^{-1}((\beta, s)) = \left(\frac{6}{m_u} \cdot \beta, \frac{\cos(\pi/m_u)}{\cos(\pi/6)} \cdot s \right), \tag{2}$$

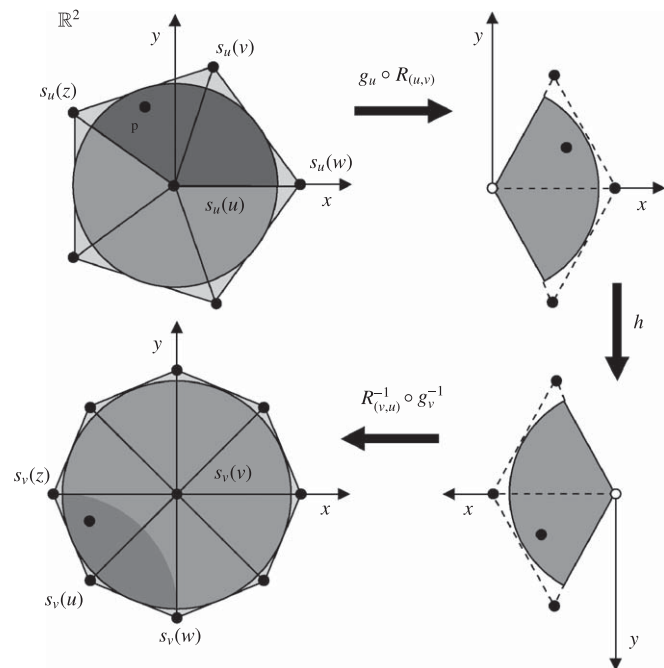where $(\beta, s) = \Pi(q)$ are the polar coordinates of q.

Fig. 5. The action of $g_{(u,v)}$ upon a point $p \in (C_u - \{(0,0)\})$.

Let $h : \mathbb{R}^2 \to \mathbb{R}^2$ be the function

$$h(p) = h((x,y)) = (1 - x, -y), \tag{3}$$

for every point $p \in \mathbb{R}^2$ with rectangular coordinates (x, y). Function h is a "double" reflection: $p = (x, y)$ is reflected over the line $x = 0.5$ and then over the line $y = 0$.

For any two vertices u, v of $\mathcal{T}$ such that $[u, v]$ is an edge of $\mathcal{T}$, let

$$g_{(u,v)} : C_u - \{(0,0)\} \to g_{(u,v)}(C_u - \{(0,0)\})$$

be the composite function given by

$$g_{(u,v)}(p) = R_{(v,u)}^{-1} \circ g_v^{-1} \circ h \circ g_u \circ R_{(u,v)}(p), \tag{4}$$

for every $p \in C_u - \{(0,0)\}$, where $R_{(u,v)}$ is a rotation around $(0,0)$ that identifies the edge $[s_u(u) = u', s_u(v)]$ of T_u with its edge $[u', u_0']$. Likewise, $R_{(v,u)}^{-1}$ is a rotation around $(0,0)$ that identifies the edge $[s_v(v) = v', v_0']$ of T_v with its edge $[v', v_j']$, where $j \in \{0, 1, \ldots, m_v - 1\}$ and $s_v(u) = v_j'$. Fig. 5 shows the action of $g_{(u,v)}$ upon a point $p \in C_u - \{(0,0)\}$.

Function $g_{(u,v)}$ also has the following interpretation: it maps a lens-shaped subset of a sector, A, of C_u onto a lens-shaped subset

of a sector, B, of C_v. These two sectors are closely related. Let w and z be the two vertices of $\mathscr{T}$ such that $[u, v, w]$ and $[u, v, z]$ are the two triangles of $\mathscr{T}$ sharing the edge $[u, v]$. Then, sector A is the circular sector of C_u contained in the quadrilateral $[s_u(u) = u', s_u(w), s_u(v), s_u(z)]$, while sector B is the circular sector of C_v contained in the quadrilateral $[s_v(v) = v', s_v(z), s_v(u), s_v(w)]$. Function $g_{(u,v)}$ is also a bijection, and its inverse, $g_{(u,v)}^{-1}$, is equal to the function $g_{(v,u)}$:

$$g_{(v,u)}(q) = R_{(u,v)}^{-1} \circ g_u^{-1} \circ h \circ g_v \circ R_{(v,u)}(q), \qquad (5)$$

for every $q \in C_v - \{(0,0)\}$. Function $g_{(u,v)}$ plays a crucial role in the definitions of gluing domains and transition functions.

Definition 4. For any $u, v \in I$, the *gluing domain* Ω_{uv} is defined as

$$\Omega_{uv} = \begin{cases} \Omega_u & \text{if } u = v, \\ g_{(v,u)}(\Omega_v) \cap \Omega_u & \text{if } [u, v] \in \mathscr{T}, \\ \emptyset & \text{otherwise}. \end{cases}$$

Although it is not obvious, the above definition of gluing domain satisfies condition 2 of Definition 1 [27]. In particular, the fact that $\Omega_{uv} = \emptyset$ if and only if $\Omega_{vu} = \emptyset$ is crucial to defining transition functions in a consistent manner. In what follows we give the formal definition of a transition function in our construction:

Definition 5. Let K be the index set

$$K = \{(u, v) \in I \times I | \Omega_{uv} \neq 0\}.$$

Then, for any pair $(u, v) \in K$, the *transition function*,

$$\varphi_{vu} : \Omega_{uv} \to \Omega_{vu},$$

is such that, for every $p \in \Omega_{uv}$, we let $\varphi_{vu}(p) = g_{(u,v)}(p)$ if $u \neq v$ and $\varphi_{vu}(p) = p$ otherwise.

Fig. 6 illustrates Definition 5.

It is important to emphasize that our transition functions are bijective and C^∞-continuous, as function g_{uv} is defined as a composition of C^∞-continuous, bijective functions. In addition, they satisfy condition 3 of Definition 1 [27].

4.2. Building parametrizations

Let $\mathscr{G}$ be a set of gluing data built from a triangle mesh, $\mathscr{T}$. Our goal now is to define a family of parametrizations, $\{\theta_u\}_{u \in I}$, from $\mathscr{G}$. To that end, we assume that we are given a surface, $S' \subset \mathbb{R}^3$, that approximates $|\mathscr{T}|$. More specifically, we assume that S' is the union of finitely many parametric surface patches, $b_\sigma : \mathbb{R}^2 \to \mathbb{R}^3$,

$$S' = \bigcup_{\sigma \in \mathscr{T}} b_\sigma(\triangle),$$

each of which is associated with a triangle, σ, of $\mathscr{T}$ and defined in the same affine frame, $\triangle \subset \mathbb{R}^2$. In addition, we require S' be at least C^0-continuous. We can view S' as describing the geometry
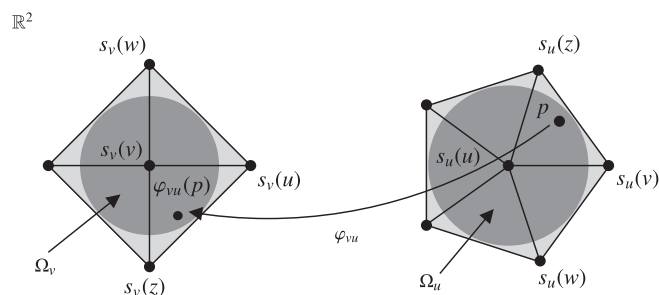
we want to locally approximate with the parametrizations. To define each parametrization θ_u, we specify a family, $\{\psi_u\}_{u \in I}$, of shape functions and a family, $\{\gamma_u\}_{u \in I}$, of weight functions.

Definition 6. For each $u \in I$, we define the *shape function*,

$$\psi_u : \square_u \subset \mathbb{R}^2 \to \mathbb{R}^3,$$

associated with Ω_u as the Bézier surface patch of bi-degree (m, n),

$$\psi_u(p) = \sum_{0 \leqslant j \leqslant m} \sum_{0 \leqslant k \leqslant n} b_{j,k}^u \cdot B_j^m(x) \cdot B_k^n(y),$$

where $\square_u = [-L, L]^2$, with $L = \cos(\pi/m_u)$, (x, y) are the coordinates of $p \in \square_u$, $\{b_{j,k}^u\} \subset \mathbb{R}^3$ are the *control points*, and

$$B_i^l(t) = \binom{l}{i} \left(\frac{L-t}{2 \cdot L} \right)^{l-i} \left(\frac{t+L}{2 \cdot L} \right)^i$$

is the i-th Bernstein polynomial of degree l *over the interval* $[-L, L] \subset \mathbb{R}$, for every $i \in \{0, 1, \ldots, l\}$. We let the bi-degree, (m, n), of ψ_u be $(m_u + 1, m_u + 1)$, where m_u is the valence of u.

The controls points are determined by solving a least squares fitting problem. In particular, $\{b_{j,k}^u\}$ is the family of control points that uniquely defines a Bézier patch of bi-degree (m, n) (i.e., ψ_u) which best fits (*in a least squares sense*) a finite set, P, of pairs, (q, p), of points, where q belongs to P_u and p belongs to the surface S'. We compute P iteratively by starting with $P = \emptyset$ and then proceeding as follows:

- We uniformly sample the domain of ψ_u (i.e., the quadrilateral $\square_u = [-L, L]^2$) to generate a set, $Q \subset P_u$, with $4 \cdot (m_u + 1)^2$ points. Note that $\square_u$ is the smallest quadrilateral that contains Ω_u. Note also that a uniform sampling of $\square_u$ will contain points that are not in P_u. These points are not placed into Q.
- For each point $q \in Q$, we find the triangle τ of $\mathscr{T}$ such that q is contained in the triangle $s_u(\tau)$ of T_u. Then, we compute the barycentric coordinates, (λ, v, η), of q with respect to $s_u(\tau)$ and use these coordinates to compute a point, $r = \lambda \cdot a + v \cdot b + \eta \cdot c$, in $\triangle = [a, b, c]$, where $\triangle$ is the common affine frame of all parametric patches defining S'. Finally, we compute $b_\tau(r)$, let $p = b_\tau(r)$, and add the pair, (q, p), to P. Fig. 7 illustrates the computation of q and p.

Once P is computed, we use a standard least squares fitting procedure to compute $\{b_{j,k}^u\}$ (see [1, p. 278]). To define the family, $\{\gamma_u\}_{u \in I}$, of weight functions, we first specify a scalar function. For
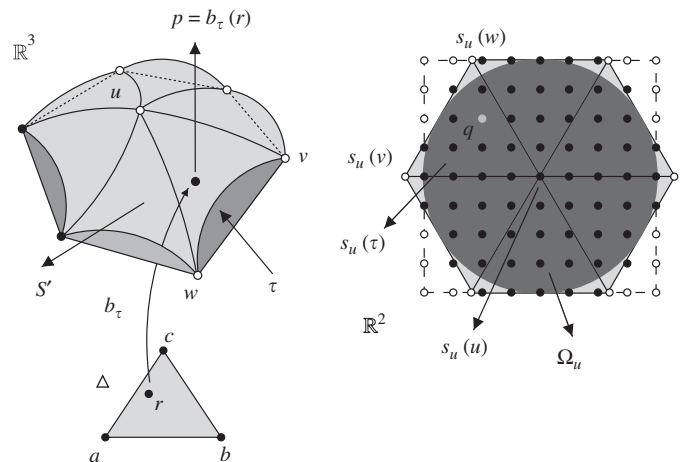

Fig. 6. Illustration of Definition 5.

Fig. 7. Local sampling of S' (white-filled vertices are not in Q).

every $t \in \mathbb{R}$, we define

$$\xi : \mathbb{R} \to \mathbb{R}$$

as

$$\xi(t) = \begin{cases} 1 & \text{if } t \leqslant H_1, \\ 0 & \text{if } t \geqslant H_2, \\ 1/(1 + e^{2 \cdot s}) & \text{otherwise,} \end{cases} \qquad (6)$$

where H_1, H_2 are constant, with $0 < H_1 < H_2 < 1$,

$$s = \left(\frac{1}{\sqrt{1 - H}} \right) - \left(\frac{1}{\sqrt{H}} \right) \quad \text{and} \quad H = \left(\frac{t - H_1}{H_2 - H_1} \right).$$

Fig. 8 shows a plot of function $\xi(t)$, for t in $[0, 1] \subset \mathbb{R}$. Note that $\xi(t)$ is constant for $t \leqslant H_1$ and $t \geqslant H_2$, and it is strictly decreasing when t varies from H_1 to H_2. Function $\xi(t)$ is C^∞, and its i-th derivative, $D^i \xi(t)$, vanishes for $t \leqslant H_1$ and $t \geqslant H_2$, and it is non-zero for $t \in (H_1, H_2) \subset \mathbb{R}$.

Definition 7. For each $u \in I$, the *weight function*,

$$\gamma_u : \mathbb{R}^2 \to \mathbb{R},$$

associated with Ω_u is given by

$$\gamma_u(p) = \xi(\sqrt{x^2 + y^2}),$$

for every $p = (x, y) \in \mathbb{R}^2$, where $\sqrt{x^2 + y^2}$ is the Euclidean distance from p to the center point, $(0, 0)$, of Ω_u. The constants H_1 and H_2 (in the definition of ξ) are experimentally chosen to be $0.25 \cdot H_2$ and $\cos(\pi/m_u)$, respectively.

By construction, function γ_u is positive for all points inside its *support*, $supp(\gamma_u)$, which is the p-domain Ω_u. Note that γ_u attains its maximum, which is equal to 1, at $p = (0, 0)$ and in the neighborhood of p given by $\{q \in \Omega_u | \|p - q\| < H_1\}$. Moreover, function γ_u decreases as p moves toward the boundary of Ω_u and vanishes outside Ω_u. This is because $\|p - q\| \geqslant H_2$, for every point $q \in \mathbb{R}^2$ on the boundary of Ω_u or outside it. So, γ_u is non-negative and its support, $supp(\gamma_u) = \Omega_u$, is compact. Finally, we can show that function γ_u is also C^∞ [27].

Definition 8. For each vertex $u \in I$, the *parametrization*, $\theta_u : \Omega_u \to \theta_u(\Omega_u) \subset \mathbb{R}^2$, associated with Ω_u is given by

$$\theta_u(p) = \sum_{v \in J_u(p)} \omega_{vu}(p) \times (\psi_v \circ \varphi_{vu}(p)), \qquad (7)$$

for every $p \in \Omega_u$, where

$$\omega_{vu}(p) = \frac{\gamma_v \circ \varphi_{vu}(p)}{\sum_{w \in J_u(p)} \gamma_w \circ \varphi_{wu}(p)} \qquad (8)$$
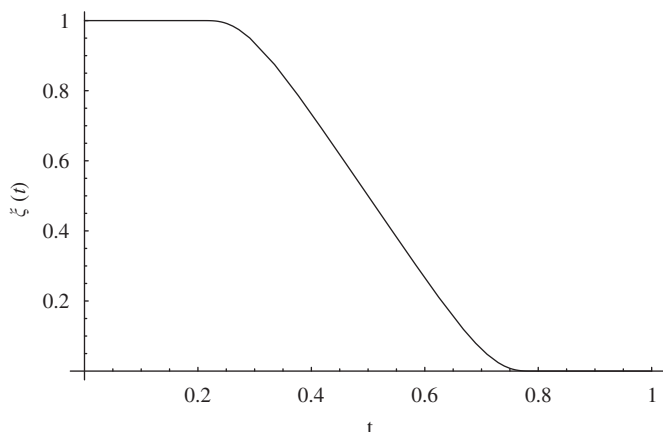

Fig. 8. Plot of $\xi(t)$ for $t \in (0, 1) \subset \mathbb{R}$, using $H_1 = 0.2$ and $H_2 = 0.8$.

and

$$J_u(p) = \{v | p \in \Omega_{uv}\} \subset I.$$

Note that $J_u(p)$, for $p \in \Omega_u$, must contain vertex u and one or two more vertices (as at most two p-domains can be glued to Ω_u at p). So, the term $\psi_v \circ \varphi_{vu}(p)$ in Eq. (7) can be viewed as the contribution of ψ_v to the position of $\theta_u(p)$. This contribution has a "weight": $\omega_{vu}(p)$. By construction, the weights are all non-negative and they also add up to 1. So, $\theta_u(p)$ is the result of a convex combination of the points $\psi_v \circ \varphi_{vu}(p)$, for all $v \in J_u(p)$. The reason to define θ_u as above is that we are guaranteed to satisfy

$$\theta_u(p) = \theta_v(\varphi_{vu}(p)),$$

for every $v \in J_u(p)$, which in turn guarantees that the union set $S = \bigcup_{u \in I} \theta_u(\Omega_u)$ is the image of a PPS (see Definition 2). The above condition is extremely unlikely to be satisfied by the shape functions ψ_u and ψ_v. The technique we used to define θ_u is based on the concept of *partition of unity*, which is well known in mathematics and also crucial to certain methods for reconstructing implicit surfaces from point sets [29].

5. Implementation and results

To implement our manifold-based construction, we augmented a simple object-oriented, topological data structure, such as a doubly connected edge list (DCEL) [30], to store the information about the set of gluing data, $\mathscr{G}$, and the family of parametrizations, $\{\theta_u\}_{u \in I}$. It is worth mentioning that there is no need to compute and store p-domains, gluing domains, P-polygons and their associated triangulations. All we need to define the differential structure of a PPS can be derived from the topological information of $\mathscr{T}$: the valence, m_v, of each vertex, v, and a cyclic ordering of the edges incident to v. Transition functions, shape functions, and

Table 1
Mesh model identifier (first column) and the number of vertices (second column), edges (third column), faces (fourth column), holes (fifth column), and connected components (sixth column) of the mesh.

Model ID	n_v	n_e	n_f	n_h	n_C
1	172	512	344	1	1
2	50	144	96	0	1
3	3,674	11,016	7,344	0	1
4	60,880	183,636	122,424	173	7

Table 2
CPU time in milliseconds for the construction of the PPS surfaces from the models in the first column and the approximated surfaces in the second column.

Model ID	Approximated surface	CPU time (ms)
1	PN triangle	540
1	Loop	577
2	PN triangle	1971
2	Loop	2112
3	PN triangle	41,160
3	Loop	44,274
4	PN triangle	679,588
4	Loop	735,221

The timing was measured on a Dell Precision 670 with Duo Pentium Xeon 3.2 GHz processors (single-core), 3 Gb RAM, and running Fedora core 9.
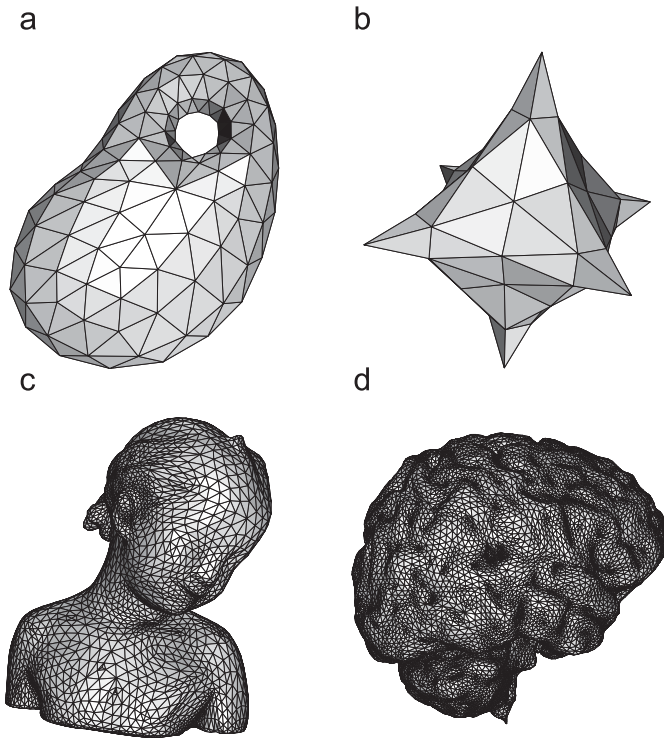
a

b

c

d

Fig. 9. Mesh models (a) 1, (b) 2, (c) 3, and (d) 4 from Table 1.

weight functions become "methods" associated with the edges and vertices of the data structure. So, although our construction description may seem complicated, its implementation is fairly simple.

The input to our implementation consists of $\mathcal{T}$ and S'. In our experiments, we defined the surface S' either as a PN triangle surface [31] or as a Loop subdivision surface [32]. In the latter case, we replaced the function b_σ with the algorithm for exact evaluation of Loop subdivision surfaces at any parameter point of its base mesh, $\mathcal{T}$ (see [33]).

We ran the aforementioned implementation on the mesh models shown in Table 1. For each mesh, we generated two PPSs, one of which approximates a PN triangle surface defined from the mesh, while the other one approximates a Loop subdivision surface also defined from the same mesh.

Table 2 shows the CPU time for the construction of each PPS, which is highly dominated by the least squares procedure that computes the control points of the shape functions. This procedure is executed n_v times, where n_v is the number of vertices of the input mesh model. Each execution solves a system of about $4 \cdot (m_u + 1)^2$ linear equations using LU decomposition and substitution, where m_u is the valence of the vertex associated with the shape function. Later, we used a procedure for placing a point on a PPS to sample the PPSs in a triangle midpoint subdivision manner [27]. We did the same for sampling the corresponding PN triangles and subdivision surfaces.

Fig. 9 shows the mesh models in Table 1. Figs. 10–13 show Gaussian curvature plots for the PN triangle, Loop subdivision, and PPSs in Table 2. These plots demonstrate two important features of our surfaces. Firstly, they show that the image of our PPSs "mimics" closely the shape of the PN triangle or Loop subdivision
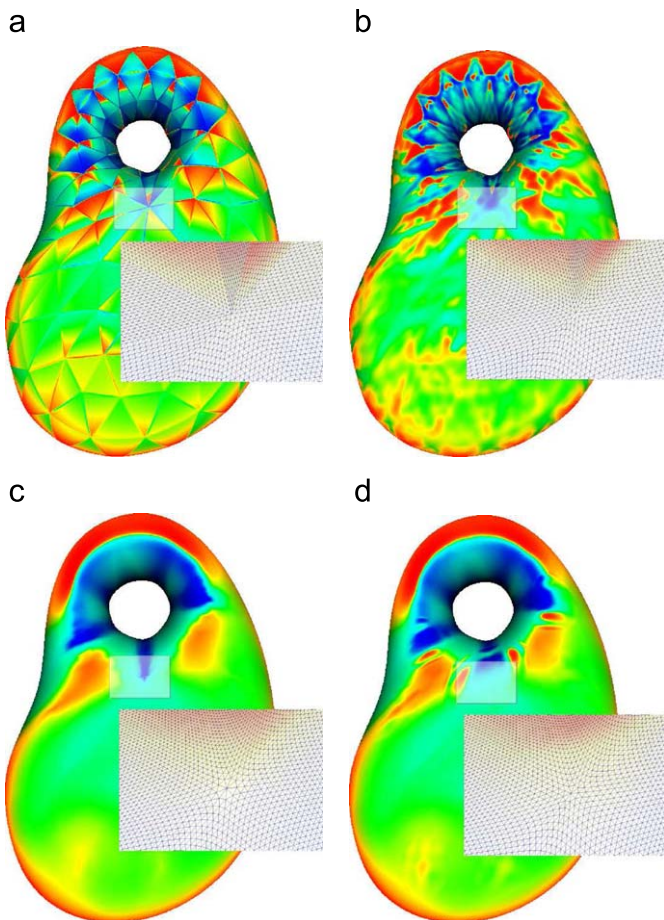
a

b

c

d

Fig. 10. Curvature plots for the surfaces generated from mesh model 1: (a) PN triangle; (b) PPS from the surface in (a); (c) Loop; and (d) PPS from the surface in (c).
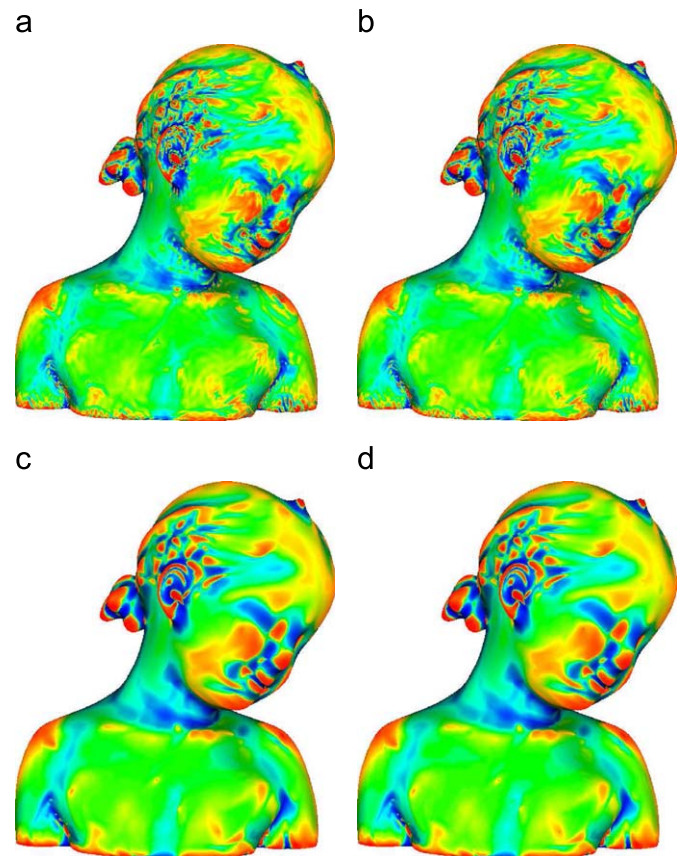
a

b

c

d

Fig. 11. Curvature plots for the surfaces generated from mesh model 3: (a) PN triangle; (b) PPS from the surface in (a); (c) Loop; and (d) PPS from the surface in (c).
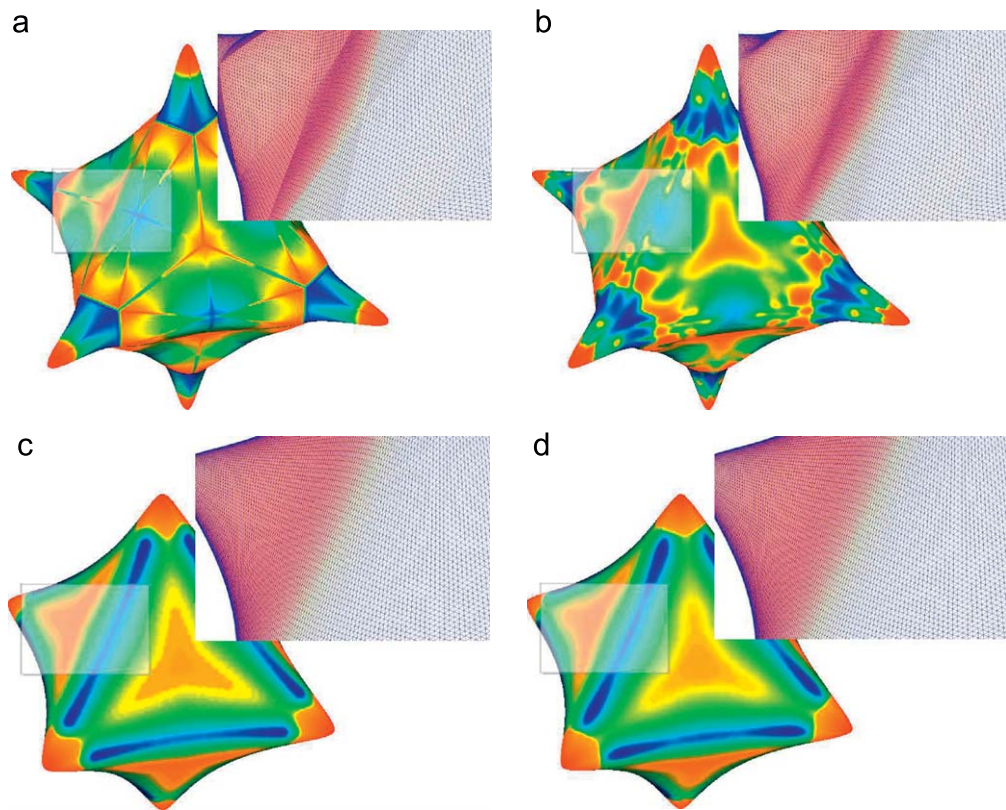
Fig. 12. Curvature plots for the surfaces generated from mesh model 2: (a) PN triangle; (b) PPS from the surface in (a); (c) Loop; and (d) PPS from the surface in (c).
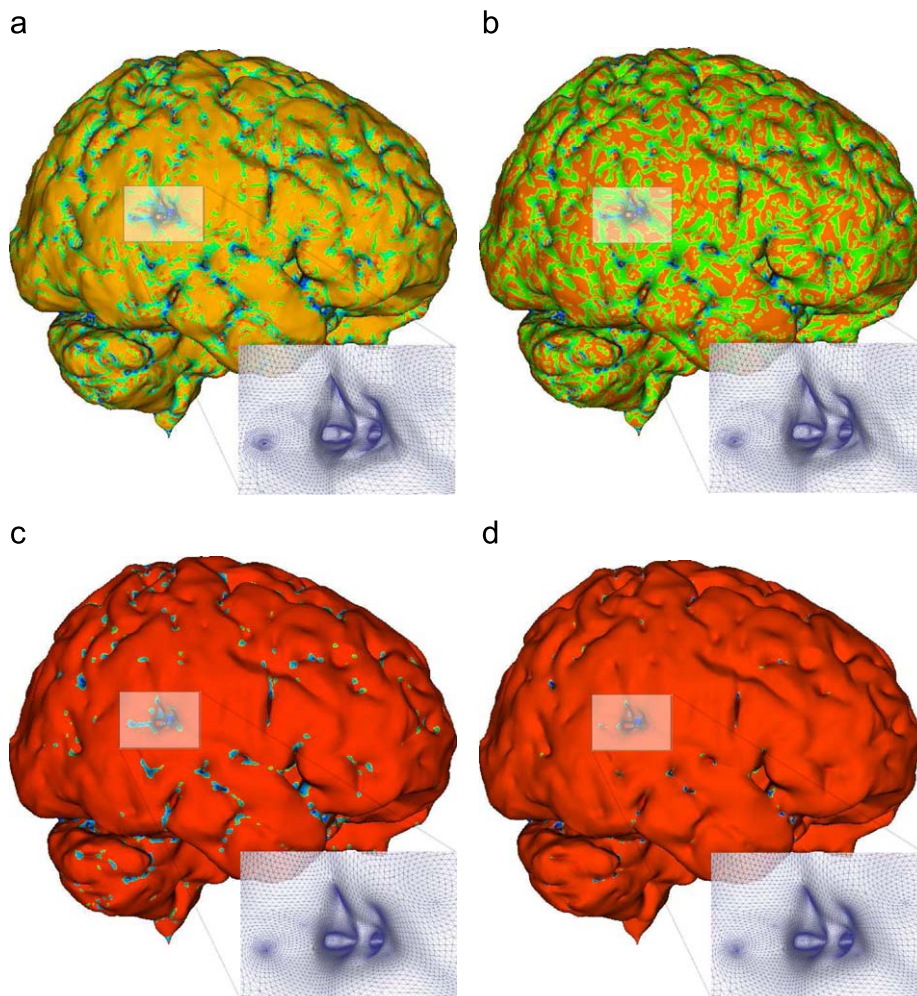

Fig. 13. Curvature plots for the surfaces generated from mesh model 4: (a) PN triangle; (b) PPS from the surface in (a); (c) Loop; and (d) PPS from the surface in (c).

surface being approximated, which are somewhat different from each other. Secondly, they also show the smoothing effect of the PPSs around the vertices and edges of the PN triangles surfaces and around the so-called extraordinary vertices of the Loop's scheme (i.e., mesh vertices not incident to six edges). In general, PN triangles surfaces are only C^0-continuous around mesh vertices and edges, while Loop subdivision surfaces are C^2 everywhere, except around extraordinary vertices where they are only C^1.

6. Conclusions and ongoing work

In this article we have introduced a new manifold-based construction for fitting a smooth surface to a triangle mesh of arbitrary topology. Our construction combines in the same framework most of the best features of previous constructions, and thus it fills the gap left by other methods. In fact, the manifold structure produced by our construction is more compact and effective than the ones in [15,16,19], because it has only one type of p-domain and transition function, the gluing domains are larger, and the number of p-domains is smaller. Like the construction in [17], ours produces C^∞-continuous surfaces and is very flexible in ways of defining their geometry. However, different from the construction in [17], ours generates surfaces from triangle meshes, rather than quadrilateral meshes, and the surfaces are contained in the convex hull of all control points used to define their geometry. Finally, unlike the surfaces produced by the triangle-based constructions in [18,24,19], the ones produced by our construction are not given by purely (rational) polynomial functions. However, our surfaces are free of singular points, and thus they do not present the visual artifacts caused by the hole-filling techniques used by [18,24] to deal with those points. Our construction is also based on a solid theoretical framework, which is an improvement upon the one in [15] and ensures the construction correctness. In addition, we provided experimental examples and concrete evidences of the effectiveness of our construction.

We are currently working on the problem of adaptively fitting C^∞ surfaces to dense triangle meshes. To this end, we are developing a new solution that closely approximates meshes with a very large number of vertices by a smooth PPS containing a small number of charts. We also plan to extend this adaptive fitting algorithm to generate a hierarchical manifold structure that can represent surfaces in multiresolution. In addition, we intend to further investigate the existence of (rational) polynomial transition functions that can replace the ones currently used by our construction (without requiring us to change the construction gluing and p-domains).

References

[1] Farin G. Curves and surfaces for CAGD: a practical guide. 5th ed. Los Altos, CA: Morgan-Kaufmann; 2002.
[2] Greiner G, Seidel H-P. Modeling with triangular B-splines. IEEE Computer Graphics and Applications 1994;14(2):56–60.
[3] Prautzsch H, Umlauf G. Parameterization of triangular g^k spline surfaces of low degree. ACM Transactions on Graphics 2006;25(4):1281–93.
[4] Catmull E, Clark J. Recursively generated B-spline surfaces on arbitrary topological surfaces. Computer-Aided Design 1978;10(6):350–5.
[5] Doo D, Sabin M. Behaviour of recursive division surfaces near extraordinary points. Computer-Aided Design 1978;10(6):356–60.
[6] Loop CT. Smooth subdivision surfaces based on triangles. Master's thesis, Department of Mathematics, University of Utah, Salt Lake City, Utah, USA; 1987.
[7] Dyn N, Levin D, Gregory JA. A butterfly subdivision scheme for surface interpolation with tension control. ACM Transactions on Graphics 1990; 9(2):160–9.
[8] Peters J, Reif U. The simplest subdivision scheme for smoothing polyhedra. ACM Transactions on Graphics 1997;16(4):420–31.
[9] Kobbelt L. $\sqrt{3}$ subdivision. In: Proceedings of the 27th annual conference on computer graphics and interactive techniques (SIGGRAPH '00). New Orleans, LA, USA, 2000. p. 103–12.
[10] Velho L, Zorin D. 4–8 subdivision. Computer Aided Geometric Design 2001; 18(5):397–427.
[11] Peters J, Reif U. Shape characterization of subdivision surfaces—basic principles. Computer Aided Geometric Design 2004;21(6):585–99.
[12] Karciauskas K, Peters J, Reif U. Shape characterization of subdivision surfaces—case studies. Computer Aided Geometric Design 2004;21(6): 601–14.
[13] Prautzsch H, Reif U. Degree estimates for C^k piecewise polynomial subdivision surfaces. Advances in Computational Mathematics 2004;10(2):209–17.
[14] Reif U. A degree estimate for subdivision surfaces of higher regularity. Proceedings of the American Mathematical Society 2006;124(7):2167–74.
[15] Grimm CM, Hughes JF. Modeling surfaces of arbitrary topology using manifolds. In: Proceedings of the 22nd ACM annual conference on computer graphics and interactive techniques (SIGGRAPH 95). ACM, 1995. p. 359–68.
[16] Navau JC, Pla-Garcia N. Modeling surfaces from meshes of arbitrary topology. Computer Aided Geometric Design 2000;7(1):643–71.
[17] Ying L, Zorin D. A simple manifold-based construction of surfaces of arbitrary smoothness. ACM Transactions on Graphics 2004;23(3):271–5.
[18] Gu X, He Y, Qin H. Manifold splines. Graphical Models 2006;68(3):237–54.
[19] Vecchia GD, Jüttler B, Kim M-S. A construction of rational manifold surfaces of arbitrary topology and smoothness from triangular meshes. Computer Aided Geometric Design 2008;25(9):801–15.
[20] Grimm CM, Zorin D. Surface modeling and parameterization with manifolds. In: ACM SIGGRAPH 2006 courses (SIGGRAPH '06). New York, NY, USA: ACM Press; 2006. p. 1–81.
[21] Grimm CM, Crisco JJ, Laidlaw DH. Fitting manifold surfaces to three-dimensional point clouds. Journal of Biomechanical Engineering 2002;124(1): 136–40.
[22] Navau JC, Pla-Garcia N, Vigo-Anglada M. A generic approach to free form surface generation. In: Proceedings of the 2002 ACM symposium on solid modeling (SM'02), 2002. p. 35–44.
[23] Milnor J, Stasheff JD. Characteristic classes. Princeton, NJ: Princeton University Press; 1974 [vol. 76 of Annals of Mathematics Studies].
[24] Gu X, He Y, Jin M, Luo F, Qin H, ng Tung Yau S. Manifold splines with single extraordinary point. Computer-Aided Design 2008;40(6):676–90.
[25] Botsch M, Pauly M, Rössl C, Bischoff S, Kobbelt L. Geometric modeling based on triangle meshes. In: SIGGRAPH course notes. ACM, 2006.
[26] Berger M, Gostiaux B. Differential geometry, manifolds, curves, and surfaces. Berlin: Springer; 2006 [vol. 115 of GTM].
[27] Siqueira M, Xu D, Gallier J. Construction of c^∞ surfaces from triangular meshes using parametric pseudo-manifolds. Technical Report, University of Pennsylvania ⟨http://repository.upenn.edu/cis_reports/877⟩; 2008.
[28] Grimm CM. Modeling surfaces of arbitrary topology using manifolds. PhD thesis, Department of Computer Science, Brown University, Providence, RI, USA; 1996.
[29] Ohtake Y, Belyaev A, Alexa M, Turk G, Seidel H-P. Multi-level partition of unity implicits. ACM Transactions on Graphics 2003;22(3):463–70.
[30] de Berg M, van Kreveld M, Overmars M, Schwarzkopf O. Computational geometry: algorithms and applications. 2nd ed. Berlin: Springer; 2000.
[31] Vlachos A, Peters J, Boyd C, Mitchell JL. Curved PN triangles. In: Proceedings of the ACM symposium on interactive 3D graphics. NC, USA: Research Triangle Park; 2001. p. 159–66.
[32] Loop CT. A G^1 triangular spline surface of arbitrary topological type. Computer Aided Geometric Design 1994;11(3):303–30.
[33] Stam J. Evaluation of Loop subdivision surfaces. In: ACM SIGGRAPH 1999 courses (SIGGRAPH '99). New York, NY, USA: ACM Press; 1999. p. 1–15.